AD-A045 586 ROME AIR DEVELOPMENT CENTER GRIFFISS AFB N Y F/G 1/4
SLOTTED WAVEGUIDE SHAPED BEAM ANTENNA AT KU BAND.(U)
JUN 77 R V MCGAHAN
UNCLASSIFIED RADC-TR-77-205 NL

1 OF 1
AD A045586

END
DATE FILMED
11-77
DDC

RADC-TR-77-205
IN-HOUSE REPORT
JUNE 1977

# Slotted Waveguide Shaped Beam Antenna at Ku Band

ROBERT V. McGAHAN





ROME AIR DEVELOPMENT CENTER
AIR FORCE SYSTEMS COMMAND
GRIFFISS AIR FORCE BASE, NEW YORK 13441

Title of Report: Slotted Waveguide Shaped Beam Antenna At Ku Band

This Technical Report has been reviewed and approved for publication:

APPROVED:

Edward E. Altshuler

EDWARD E. ALTSHULER, Chief
Tropospheric Propagation Branch
Electromagnetic Sciences Division

APPROVED:

Allan C. Schell

ALLAN C. SCHELL
Acting Chief
Electromagnetic Sciences Division

FOR THE COMMANDER:

Plans Office John P. Huss

# *MISSION*
# *of*
# *Rome Air Development Center*

*RADC plans and conducts research, exploratory and advanced development programs in command, control, and communications ($C^3$) activities, and in the $C^3$ areas of information sciences and intelligence. The principal technical mission areas are communications, electromagnetic guidance and control, surveillance of ground and aerospace objects, intelligence data collection and handling, information system technology, ionospheric propagation, solid state sciences, microwave physics and electronic reliability, maintainability and compatibility.*

Printed by
United States Air Force
Hanscom AFB, Mass. 01731

Unclassified

SECURITY CLASSIFICATION OF THIS PAGE (When Data Entered)

| REPORT DOCUMENTATION PAGE | READ INSTRUCTIONS BEFORE COMPLETING FORM |
|---|---|
| 1. REPORT NUMBER: RADC-TR-77-205 | 2. GOVT ACCESSION NO. / 3. RECIPIENT'S CATALOG NUMBER |
| 4. TITLE (and Subtitle): SLOTTED WAVEGUIDE SHAPED BEAM ANTENNA AT KU BAND | 5. TYPE OF REPORT & PERIOD COVERED: In-House Report, 1 Nov 75 - 31 Aug 77 |
| | 6. PERFORMING ORG. REPORT NUMBER |
| 7. AUTHOR(s): Robert V. McGahan | 8. CONTRACT OR GRANT NUMBER(s) |
| 9. PERFORMING ORGANIZATION NAME AND ADDRESS: Deputy for Electronic Technology (RADC/ETEN), Hanscom AFB, Massachusetts 01731 | 10. PROGRAM ELEMENT, PROJECT, TASK AREA & WORK UNIT NUMBERS: PE 62702F, 46001601 |
| 11. CONTROLLING OFFICE NAME AND ADDRESS: Deputy for Electronic Technology (RADC/ETEN), Hanscom AFB, Massachusetts 01731 | 12. REPORT DATE: June 1977 |
| | 13. NUMBER OF PAGES: 16 (18 p.) |
| 14. MONITORING AGENCY NAME & ADDRESS (if different from Controlling Office): 4600 / 16 | 15. SECURITY CLASS. (of this report): Unclassified |
| | 15a. DECLASSIFICATION/DOWNGRADING SCHEDULE |

16. DISTRIBUTION STATEMENT (of this Report)

Approved for public release; distribution unlimited.

DDC RECEIVED OCT 27 1977 B

17. DISTRIBUTION STATEMENT (of the abstract entered in Block 20, if different from Report)

18. SUPPLEMENTARY NOTES

19. KEY WORDS (Continue on reverse side if necessary and identify by block number)

Inclined shunt
Ku band antennas
Shaped beam antennas
Slotted waveguide

20. ABSTRACT (Continue on reverse side if necessary and identify by block number)

A Ku band slotted waveguide antenna having a cosecant squared radiation pattern is described. The antenna was designed and constructed by means of a method utilizing displaced, inclined, shunt slots in the broad face of WR 62 waveguide. A gain of 12 dB at 15.84 GHz was measured, with crosspolarization rejection of 20 dB. Design equations and curves are included.

DD FORM 1 JAN 73 1473 EDITION OF 1 NOV 65 IS OBSOLETE

Unclassified

SECURITY CLASSIFICATION OF THIS PAGE (When Data Entered)

309050 B

## Contents



## Illustrations

## Illustrations



## Table

# Slotted Waveguide Shaped Beam Antenna at Ku Band

## 1. INTRODUCTION

This report describes work performed under Project 86820602, later changed to Project 46001601. In the course of developing the Phase Derived Navigation System (Project 46001601), a microwave landing system, the need arose for six identical beacon antennas. These beacon antennas are used to delineate the boundaries of the landing zone (runway) in question, in order that a cockpit display may be generated.

The requirement was for an antenna to produce a cosecant pattern in elevation and an omni-directional pattern in azimuth. The frequency of operation was to be 15.84 GHz. Linear polarization was desired. Since the units were to be mounted in a field environment on portable transmitters, both weight and ease of mounting were considerations.

The necessity for a shaped beam in one plane indicated either a phased array or a specially shaped reflector. This, along with the aforementioned weight and mounting problems, led to adoption of an array of slots in a waveguide.

The shaped beam desired requires a non-linear progressive phase across the array. Since equi-spaced longitudinal shunt slots can produce only linear phase distributions they were deemed inappropriate. The requirement that each

(Received for publication 16 June 1977)

slot have independently controllable phase and amplitude led to utilization of a method discussed by Maxum.[1]

This method allows the phase and amplitude of each slot to be controlled independently by inclining and displacing it appropriately. Plotting the equation describing the fields in the waveguide as a function of displacement and inclination allows a graphical solution for the position of each slot. This method is discussed in detail in Section 3.

## 2. SYNTHESIS OF ELEMENT CURRENTS

Before discussing the design of the slots, a description of the method used to determine the element currents will be presented. Since the cosecant elevation pattern was to be synthesized by an array of discrete radiators it was decided to use Schelkunoff's Method.[2,3] In this method, the desired farfield pattern is expanded in a Fourier series of M terms, where M is the number of elements in the array, and the current on the mth element is then associated with the coefficient of the mth term in the series.

Letting $M = 2N+1$, the synthesized pattern can be written as a sum of terms

$$F_D(u) = \sum_{n=-N}^{N} A_n e^{jkn\delta u} \cdot \tag{1}$$

where $\delta$ is the element spacing, k is the wave number $\frac{2\pi}{\lambda}$, and $u = \cos\theta$. The various coefficients are

$$A_n = \int_{-1}^{1} F_D(u)\, e^{-jkn\delta u}\, du \tag{2}$$

where $F_D$ is the pattern to be synthesized.

Applying this to the specific case of a linear array of uniformly spaced elements, $M = 21$ and $\delta = \lambda/2$, using the geometry of Figure 1,

---

1. Maxum, B.J. (1960) "Resonant Slots with Independent Control of Amplitude and Phase" IRE T-AP Vol. AP-8, 4:384.
2. Schelkunoff, S.A. (1943) "A Mathematical Theory of Linear Arrays," BESTJ, Vol. 22, 1:80-107.
3. Collin, R.E. and Zucker, F.J. (1969) Antenna Theory, McGraw-Hill, New York, Part 1, Chap. 7, "Antenna Pattern Synthesis."

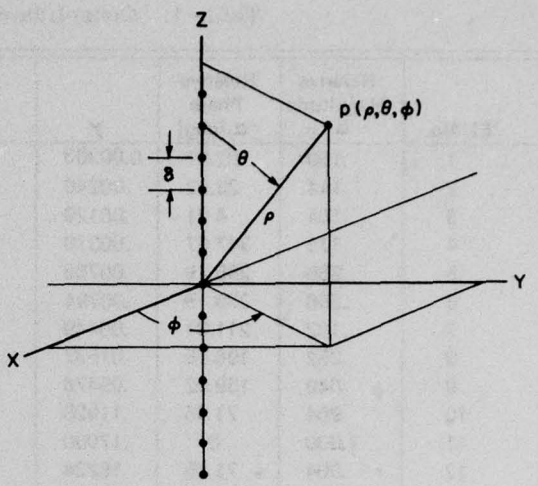


Figure 1. Coordinate System

$$A_n = \int_{-1}^{1} \frac{1}{u} e^{-jn\pi u}\, du.$$

$A_n$ is complex, with magnitude $a_n$ and phase $\alpha_n$. Denoting the region of interest as extending from $u_1$ to $u_2$

$$A_n = \int_{u_1}^{u_2} \frac{1}{u} e^{-jn\pi u}\, du = Ci(n\pi u_2) - Ci(n\pi u_1) - j[Si(n\pi u_2) - Si(n\pi u_1)]. \qquad (3)$$

Solving for 21 elements over the region $u_1 = .2$, $u_2 = .7$, corresponding to the angular range $12° \leq \theta \leq 45°$, yields the element currents listed in Table 1. Theoretical farfield patterns have been computed using these currents and are discussed in Section 4.

Table 1. Consolidated Design Results

| EL No. | Relative Magnitude a | Relative Phase α [deg] | $\gamma$ | $\left\|\frac{V}{A}\right\|$ | $\Delta x$ [inch] | $\theta$ [deg] | Resonant Length $\ell$ [inch] |
|---|---|---|---|---|---|---|---|
| 1 | .160 | 82.91 | 0.00303 | 1.048 | − .002 | 3.0 | .36 |
| 2 | .144 | 28.92 | .00246 | .944 | .013 | − 1.3 | .36 |
| 3 | .104 | 4.91 | .00129 | .628 | − .010 | .15 | .36 |
| 4 | .176 | 347.87 | .00370 | 1.157 | .017 | .7 | .361 |
| 5 | .256 | 295.19 | .00788 | 1.689 | − .011 | − 4.0 | .361 |
| 6 | .256 | 239.15 | .00794 | 1.696 | − .013 | 4.0 | .361 |
| 7 | .192 | 211.81 | .00449 | 1.275 | .016 | − 1.8 | .36 |
| 8 | .352 | 196.55 | .01532 | 2.355 | − .033 | 1.8 | .361 |
| 9 | .648 | 139.92 | .05476 | 4.453 | .051 | 8.1 | .363 |
| 10 | .904 | 71.45 | .11928 | 6.572 | .031 | −17.5 | .364 |
| 11 | 1.000 | 0 | .17090 | 7.866 | − .125 | 0 | .373 |
| 12 | .904 | − 71.45 | .16234 | 7.666 | .037 | 20.6 | .365 |
| 13 | .648 | −139.92 | .09100 | 5.740 | .066 | −10.8 | .362 |
| 14 | .352 | −196.55 | .02759 | 3.161 | − .045 | − 2.5 | .362 |
| 15 | .192 | −211.81 | .00828 | 1.731 | .022 | 2.5 | .36 |
| 16 | .256 | −239.15 | .01494 | 2.325 | − .018 | − 5.5 | .361 |
| 17 | .256 | −295.19 | .01516 | 2.343 | − .015 | 5.8 | .361 |
| 18 | .176 | −347.87 | .00722 | 1.617 | .023 | − 1.0 | .36 |
| 19 | .104 | − 4.91 | .00253 | .956 | − .014 | − .2 | .36 |
| 20 | .144 | − 28.92 | .00487 | 1.328 | .018 | 1.8 | .36 |
| 21 | .160 | − 82.11 | .00605 | 1.480 | − .003 | − 4.0 | .36 |

## 3. SLOT DESIGN PROCEDURE

The design of the slots was carried out according to the method described in Section 1. This method consists of four parts, once the synthesis of element currents is completed.

First the percentage of input power to be radiated is chosen and a coupling coefficient gamma ($\gamma$) is computed for each element in the array. The gammas account for the loss in total power as one proceeds along the array and are used to determine the displacement of each slot from the center line of the waveguide. The coupling coefficients are given by

$$\gamma_n = \frac{a_n^2 P_r}{K_M - K_n P_r} , \tag{4}$$

where $P_r$ is the percent power radiated (expressed as a decimal), $K_n$ is the running sum of the $a_n^2$:

$$K_n = \sum_{n=-N}^{n} a_n^2,$$

and $a_n$ is found from the complex element excitation

$$A_n = |A_n| e^{j\alpha n} = a_n e^{j\alpha n} .$$

As in Section 2, $M = 2N+1$ and thus

$$K_M = \sum_{-N}^{N} a_n^2.$$

Once the coupling coefficients are determined, the ratio of the slot voltage to the amplitude of the dominant mode in the waveguide can be determined by

$$\left|\frac{V}{A}\right|_n = \sqrt{Ck_o k_g \frac{b}{a} \gamma} , \tag{5}$$

where $k_o$ and $k_g$ are $2\pi/\lambda_o$ and $2\pi/\lambda_h$, respectively, and have units of radians/meter, a and b are the inside dimensions of the waveguide, and C is a constant. The value of C depends on the units of $k_o$ and $k_g$; for the given case $C = 8.22 \times 10^{-3}$, while in Maxum's paper [1], $C = 12.74$, due to the fact that therein the units of $k_o$ and $k_g$ are rad/inch.

The next step in the design procedure is to determine $\theta$, the angle of inclination, and $\Delta x$, the displacement, for each slot. The complex excitation for a slot can be expressed as a function of $\theta$ and x, where $\theta$ and x are as designated in Figure 2:

$$\frac{V}{A} = \left|\frac{V}{A}\right| e^{j\alpha} = \frac{8.1}{a} \left[ Be^{\frac{j\pi x}{a}} + De^{\frac{-j\pi x}{a}} \right] , \tag{6}$$

where

$$B = \frac{\cos\left(\frac{\pi}{2}\cos(i-\theta)\right)}{\sin(i-\theta)} , \quad D = \frac{\cos\left(\frac{\pi}{2}\cos(i+\theta)\right)}{\sin(i+\theta)} ,$$

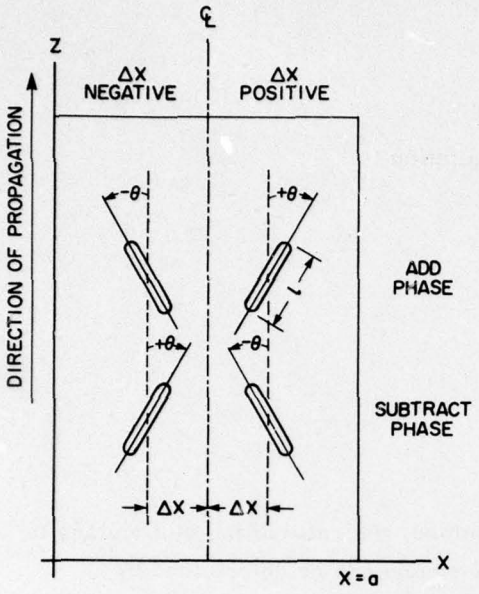


Figure 2. Slot Parameters Defined

and i is the frequency dependent angle of incidence of the propagating wave in the guide given by $i = \sin^{-1}(\lambda_o/2a)$. The phase $\alpha$ is found from the element excitation, while the magnitude ratio $|V/A|$ is determined from the coupling coefficient.

When Equation 6 is plotted, curves relating slot excitation (magnitude and phase) to slot orientation result, as in Figure 3. How well a given slot, when constructed, will perform depends on two things, the machining tolerances and the actual orientation of the slot. Slot excitations with large V/A ratios and large inclination angles are relatively insensitive to machining errors because of the steepness of the curves in these regions, but these slots are near the limits of validity of the design method. Slots with small V/A ratios and inclination angles are well within the design limitations but are much more sensitive to machining errors.

Examination of Figure 3 indicates that the range of excitation phases extends only from 0° to 90°. However any phase in the range $-180° \leq \alpha \leq 180°$ can be obtained. Use is made of the fact that the phase of the field inside a waveguide can be changed by 180° by crossing the center line perpendicularly or by moving along the guide to a point $\lambda_g/2$ away. Thus a slot excitation can be put into the proper phase range ($-180° \leq \alpha \leq 0$ or $0 \leq \alpha \leq 180°$) by moving a multiple of $\lambda_g/2$ along the guide from some reference, and crossing the center line if necessary. The proper quadrant can then be selected by choosing the sign of the inclination angle.

Using the conventional formulation of wave propagation in the positive z direction, and the geometry of Figure 2, a method of determining which of the

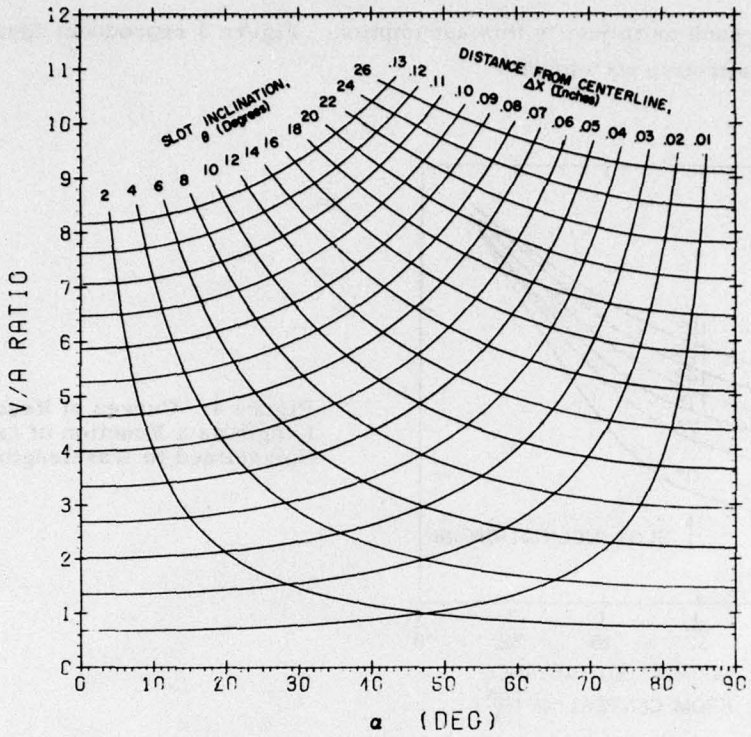


Figure 3. Design Curves Relating $\Delta x$ and $\theta$ to Slot Excitations

four possible slot orientations will put the slot excitation phase in the proper quadrant follows. Examination of the fields within the waveguide shows that a negative $\Delta x$ and a positively increasing $\theta$ produce phases which vary from 0° to +90°. This first quadrant condition is taken as the reference. A slot with negative $\Delta x$ and negatively increasing $\theta$ can have phase variations from 0° to -90°. Positive $\Delta x$ and positively or negatively increasing $\theta$ produce phase variations 180° to 90° (second quadrant) or -180° to -90° (third quadrant) respectively. The foregoing are applicable for a slot at the same z as the reference slot. When one moves along the guide, as in constructing an array, one must account for the n(180°) phase shifts incurred thereby. These conditions are summarized in Figure 2.

The fourth and final step in the design of the slots is to determine their lengths. Maxum measured the resonant lengths of slots for various combinations of $\Delta x$ and $\theta$, and interpolated the results to obtain a family of curves. Maxum's curves give slot length (l) vs $\Delta x$ and $\theta$, where l and $\Delta x$ are in inches, for WR90 waveguide at 9.375 GHz. It was reasoned that these curves could be normalized to wavelength and used at 15.84 GHz for WR62 guide and, indeed, experimental

results were such as to justify this assumption. Figure 4 reproduces Maxum's curves normalized to wavelength.

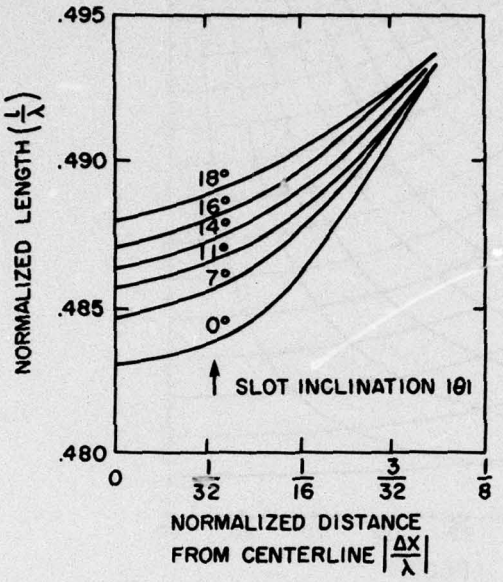


Figure 4. Curves of Resonant Slot Length as a Function of $\Delta x$ and $\theta$ Normalized to Wavelength

## 4. RADIATION PATTERNS

The synthesized element currents listed in Table 1 were used to compute theoretical farfield patterns. These patterns were computed assuming an array of collinear dipoles. The length of each dipole was $\lambda_o/2$, and the center-to-center separation was $\lambda_g/2$, where $\lambda_o$ and $\lambda_g$ are the free-space and guide wavelengths, respectively, as depicted in Figure 5.

The element pattern used was that of a slot in a ground plane.[4] When the long axis of the slot is parallel to the z-axis this pattern becomes:

$$I_{\text{slot}}(\theta) = \frac{\cos\left(\frac{\pi}{2}\sin\theta\right)}{\cos\theta} \qquad (7)$$

where $\theta$ is measured from the positive y-axis as in Figure 6. Figure 6 also shows the comparison between this element pattern and that of $\cos\theta$ over the same range.

4. Fante, R.L. and Mayhan, J.T. (1970) "Bounds on the Electric Field Outside a Radiating System - II," IEEE T-AP Vol. AP-18, 1:64.

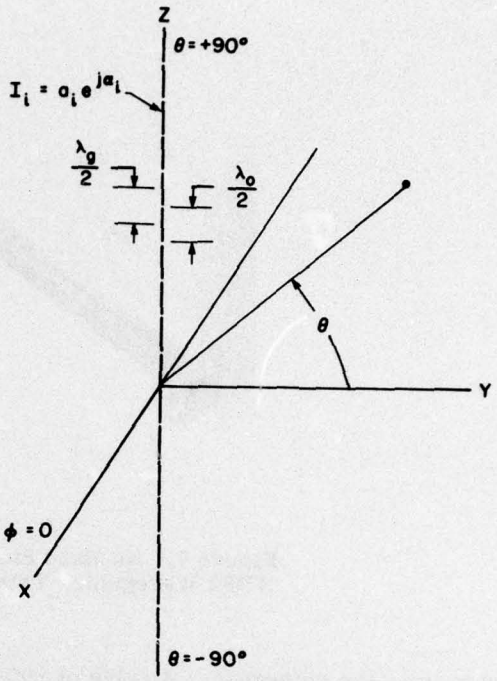


Figure 5. Geometry Used to Analyze the Slot Array

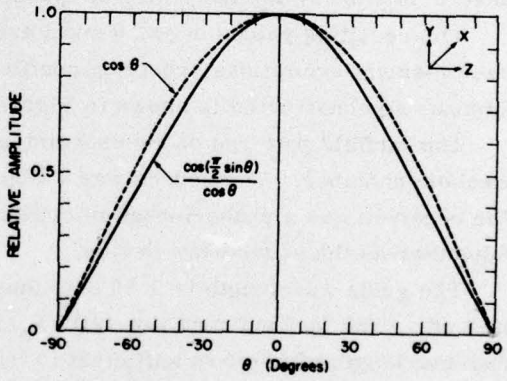


Figure 6. Element Pattern for a Slot.

Although the slots were inclined, rather than parallel to the long axis of the waveguide, and were, in general, shorter than $\lambda_o/2$ due to changes in resonance conditions, as well as being offset from the center line by varying amounts because of the magnitude requirements, these deviations were small. Therefore, they were ignored in computing theoretical farfield patterns and a common axis was assumed. The resulting pattern for the region of interest is shown in Figure 8.

The method outlined in Section 3 was used to design an array of 21 slots to produce the cosecant pattern synthesized in Section 2. The center element was

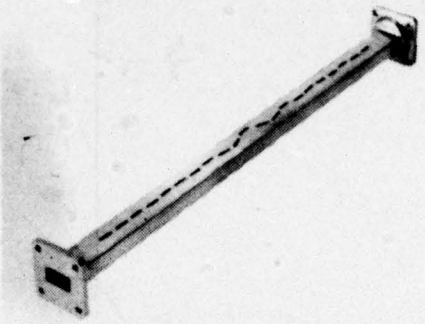

Figure 7. Ku Band Slotted Waveguide Antenna, WR62 Waveguide, Total Length = 31 cm.

chosen as the reference. A value of 50% was chosen for the power radiated. As noted in Section 1, the frequency of operation was 15.84 GHz.

The resulting values of $\Delta x$, $\theta$ and 1 are listed in Table 1 along with the synthesized element excitations, coupling coefficients ($\gamma$) and $|V/A|$ ratios. One of the antennas so constructed is shown in Figure 7.

The farfield patterns of the experimental antennas were measured in an anechoic chamber. The source was a Gunn Diode Oscillator feeding a small horn. The receiver was a phase-locked microwave measurements receiver using a bolometer as the square-law device.

The guide wavelength is 2.36 cm, thus the aperture (D) of the array is 24.8 cm. The farfield condition ($2D^2/\lambda_o$) for this antenna is 6.5 m, thus the chamber length of 9 m was sufficient to insure being in the far field.

A typical measured pattern*, taken at 15.84 GHz, is shown in Figure 9.

---

* Seven identical units were ultimately constructed by a machinist. The first unit was made with a makeshift jig and had poorer performance than the remaining six. These six had patterns which were identical to within one dB.

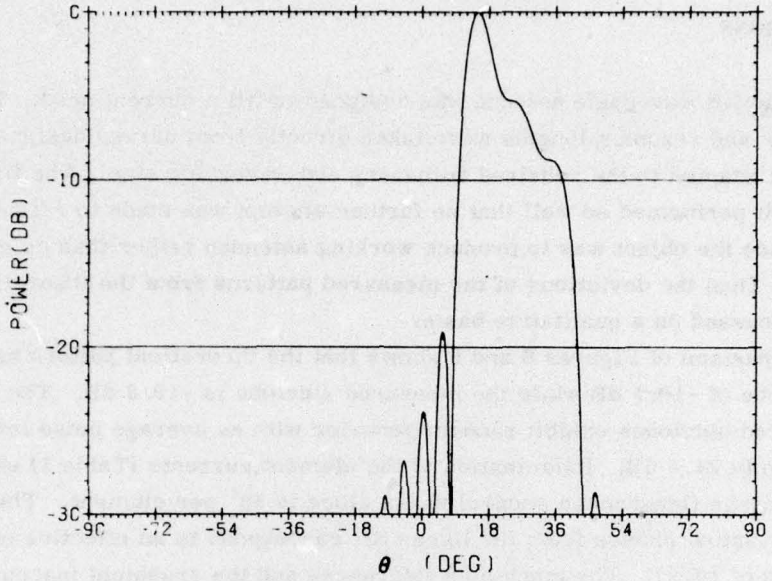


Figure 8. Theoretical Radiation Pattern of Slot Array. Frequency = 15.84 GHz

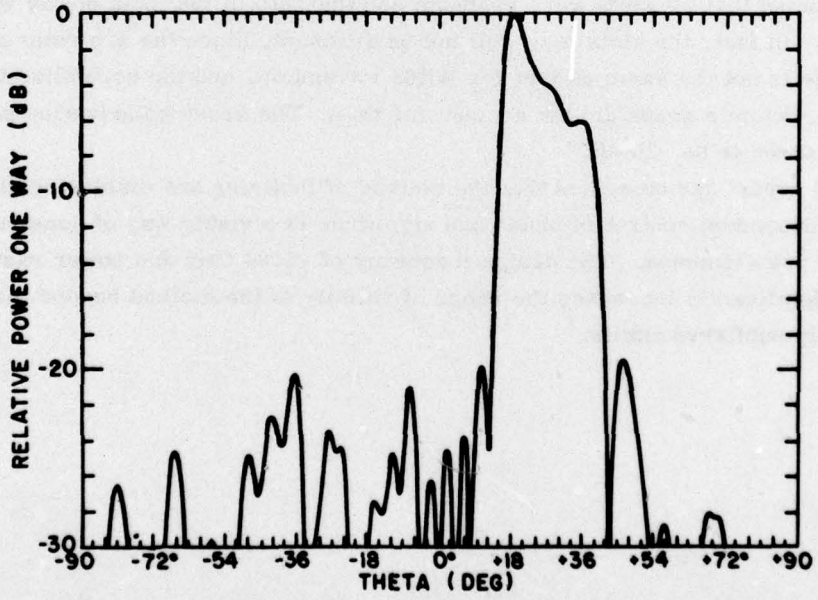


Figure 9. Measured Radiation Pattern of Ku Band Slotted Waveguide Antenna. Frequency = 15.84 GHz

## 5. CONCLUSIONS

This slotted waveguide antenna was designed to fill a current need. The slot orientations and resonant lengths were taken directly from curves designed by Maxum and adapted to the required frequency and waveguide size. The first models built performed so well that no further attempt was made to refine the theory, since the object was to produce working antennas rather than do novel research. Thus the deviations of the measured patterns from the theoretical can only be discussed on a qualitative basis.

A comparison of Figures 8 and 9 shows that the theoretical pattern has a first sidelobe of -19.1 dB while the measured sidelobe is -19.8 dB. The remaining measured sidelobes exhibit random behavior with an average noise level of approximately 24.3 dB. Examination of the element currents (Table 1) shows that the average (least mean square) phase slope is 58° per element. The deviations of the actual phases from the linear tilt correspond to an effective number of elements of 10.27. The machining tolerances and the graphical inaccuracies in the design indicate a mean square phase error of 12° per element. These values are consistent with the observed -24 dB average sidelobe level.

The measured gain of the experimental model was 12 dB. Assuming an elevation element pattern as in Section 4, Equation 7, and a cartiod azimuthal pattern $(1+\cos\phi)$, a theoretical gain of 12.8 dB was calculated. The calculated gain assumed that all slots were resonant and that 50% of the input power was radiated. In fact, the slots may well not be resonant, since the a/b ratio of WR90 waveguide is not the same as that for WR62 waveguide, and the normalization made on Maxum's graph did not account for this. The cross polarization pattern was measured to be -20 dB.

This report demonstrates that the method of inclining and displacing slots to obtain independent control of phase and amplitude is a viable way of constructing a shaped beam antenna. The design frequency of 15.84 GHz and power radiated of 50% significantly increases the range of validity of the method beyond the previously published limits.[1]

## METRIC SYSTEM

### BASE UNITS:

| Quantity | Unit | SI Symbol | Formula |
|---|---|---|---|
| length | metre | m | ... |
| mass | kilogram | kg | ... |
| time | second | s | ... |
| electric current | ampere | A | ... |
| thermodynamic temperature | kelvin | K | ... |
| amount of substance | mole | mol | ... |
| luminous intensity | candela | cd | ... |

### SUPPLEMENTARY UNITS:

| | | | |
|---|---|---|---|
| plane angle | radian | rad | ... |
| solid angle | steradian | sr | ... |

### DERIVED UNITS:

| | | | |
|---|---|---|---|
| Acceleration | metre per second squared | ... | m/s |
| activity (of a radioactive source) | disintegration per second | ... | (disintegration)/s |
| angular acceleration | radian per second squared | ... | rad/s |
| angular velocity | radian per second | ... | rad/s |
| area | square metre | ... | m |
| density | kilogram per cubic metre | ... | kg/m |
| electric capacitance | farad | F | A-s/V |
| electrical conductance | siemens | S | A/V |
| electric field strength | volt per metre | ... | V/m |
| electric inductance | henry | H | V-s/A |
| electric potential difference | volt | V | W/A |
| electric resistance | ohm | | V/A |
| electromotive force | volt | V | W/A |
| energy | joule | J | N-m |
| entropy | joule per kelvin | ... | J/K |
| force | newton | N | kg-m/s |
| frequency | hertz | Hz | (cycle)/s |
| illuminance | lux | lx | lm/m |
| luminance | candela per square metre | ... | cd/m |
| luminous flux | lumen | lm | cd-sr |
| magnetic field strength | ampere per metre | ... | A/m |
| magnetic flux | weber | Wb | V-s |
| magnetic flux density | tesla | T | Wb/m |
| magnetomotive force | ampere | A | ... |
| power | watt | W | J/s |
| pressure | pascal | Pa | N/m |
| quantity of electricity | coulomb | C | A-s |
| quantity of heat | joule | J | N-m |
| radiant intensity | watt per steradian | ... | W/sr |
| specific heat | joule per kilogram-kelvin | ... | J/kg-K |
| stress | pascal | Pa | N/m |
| thermal conductivity | watt per metre-kelvin | ... | W/m-K |
| velocity | metre per second | ... | m/s |
| viscosity, dynamic | pascal-second | ... | Pa-s |
| viscosity, kinematic | square metre per second | ... | m/s |
| voltage | volt | V | W/A |
| volume | cubic metre | ... | m |
| wavenumber | reciprocal metre | ... | (wave)/m |
| work | joule | J | N-m |

### SI PREFIXES:

| Multiplication Factors | Prefix | SI Symbol |
|---|---|---|
| 1 000 000 000 000 = $10^{12}$ | tera | T |
| 1 000 000 000 = $10^{9}$ | giga | G |
| 1 000 000 = $10^{6}$ | mega | M |
| 1 000 = $10^{3}$ | kilo | k |
| 100 = $10^{2}$ | hecto* | h |
| 10 = $10^{1}$ | deka* | da |
| 0.1 = $10^{-1}$ | deci* | d |
| 0.01 = $10^{-2}$ | centi* | c |
| 0.001 = $10^{-3}$ | milli | m |
| 0.000 001 = $10^{-6}$ | micro | μ |
| 0.000 000 001 = $10^{-9}$ | nano | n |
| 0.000 000 000 001 = $10^{-12}$ | pico | p |
| 0.000 000 000 000 001 = $10^{-15}$ | femto | f |
| 0.000 000 000 000 000 001 = $10^{-18}$ | atto | a |

* To be avoided where possible.